

Oxidative and Photochemical Stability of Ionomers for Fuel-Cell Membranes

by Svetlin Mitov^a), Olga Delmer (geb. Reifschneider)^{a)1)}, Jochen Kerres^{b)}, and Emil Roduner^{*a)}

^{a)} Institute of Physical Chemistry, University of Stuttgart, Pfaffenwaldring 55, D-70569 Stuttgart (phone: +49-711-6856-4490; fax: +49-711-6856-4495; e-mail: e.roduner@ipc.uni-stuttgart.de)

^{b)} Institute for Chemical Engineering, University of Stuttgart, Böblingerstr. 72, D-70199 Stuttgart

In memoriam Professor Hanns Fischer

To predict hydroxyl-radical-initiated degradation of new proton-conducting polymer membranes based on sulfonated polyetherketones (PEK) and polysulfones (PSU), three nonfluorinated aromatics are chosen as model compounds for EPR experiments, aiming at the identification of products of HO[•]-radical reactions with these monomers. Photolysis of H₂O₂ was chosen as the source of HO[•] radicals. To distinguish HO[•]-radical attack from direct photolysis of the monomers, experiments were carried out in the presence and absence of H₂O₂. A detailed investigation of the pH dependence was performed for 4,4'-sulfonylbis[phenol] (**SBP**), bisphenol A (=4,4'-isopropylidenebis[phenol]; **BPA**), and [1,1'-biphenyl]-4,4'-diol (**BPD**). At pH ≥ pK_A of HO[•] and H₂O₂, reactions between the model compounds and O₂^{•-} or ¹O₂ are the most probable ways to the phenoxy and 'semiquinone' radicals observed in this pH range in our EPR spectra. A large number of new radicals give evidence of multiple hydroxylation of the aromatic rings. Investigations at low pH are particularly relevant for understanding degradation in polymer-electrolyte fuel cells (PEFCs). However, the chemistry depends strongly on pH, a fact that is highly significant in view of possible pH inhomogeneities in fuel cells at high currents. It is shown that also direct photolysis of the monomers leads to 'semiquinone'-type radicals. For **SBP** and **BPA**, this involves cleavage of a C–C bond.

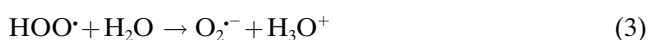
Introduction. – In the past years, there has been a tremendous acceleration in research devoted to nonfluorinated polymer membranes, both as competitive alternatives to commercial perfluorosulfonic acid membranes operating in the same temperature range and with the objective of extending the range of operation of polymer fuel cells toward those more generally occupied by phosphoric acid fuel cells [1]. Consequently, much effort has focused on the development of alternative proton-exchange membranes for PEFCs (polymer-electrolyte fuel cells) and DMFCs (direct methanol fuel cells), in particular with the aim of increasing their temperature of operation. Important advantages in terms of water management, increased proton conductivity, and CO tolerance in fuel cells can be gained by operating at higher temperature, typically at *ca.* 120°. This operating temperature imposes additional stringent requirements in terms of membrane stability in a highly oxidative environment. There are few nonfluorinated membrane materials appropriate for fuel cell applications at temperatures above 80°, and they are made up of polyaromatic or polyheterocyclic repeat units.

¹⁾ Present address: Max Planck Institute for Solid State Research, Heisenbergstr. 1, D-70569 Stuttgart.

Examples include polysulfones (PSU), polyetherketone (PEK), polybenzimidazole (PBI), polyethersulfone, polyphenylquinoxaline, polyetherimides, *etc.* Furthermore, polymer blending is a potentially versatile way of tuning the properties to those desirable for fuel-cell application. For instance, sulfonated PEK and PSU have been used in blends with PBI, as well as with more weakly basic components such as polyetherimine, polyethylenimine and poly(4-vinylpyridine) [1][2]. A general problem of most approaches for development of novel, nonfluorinated fuel-cell membranes is that these polymers and membranes are developed *via* the trial-and-error principle. Therefore, there is a strong need for the preparation of novel fuel-cell membranes following a more fundamental approach, including subsequent investigation of the chemical and thermal stability of the monomers, polymers, membranes, and membrane–electrode assemblies (MEAs).

To ensure long-term durability of the new materials, investigations of possible degradation mechanisms are necessary. HO• and HOO• radicals originating from oxygen diffusion through the membrane and incomplete reduction at the fuel-cell anode are held responsible for these degradation reactions [3][4]. Hydroxyl and hydroperoxyl radicals are regular intermediates of the cathode reaction. This is unproblematic as long as they remain attached to the catalyst surface. The intermediate of oxygen reduction, hydrogen peroxide, can be formed in sufficient amounts on the catalyst surface at the cathode side of the cell [5]. In the presence of noble metals and at elevated temperatures, H₂O₂ decays into hydroxyl radicals HO• which attack the membrane [6]. Because of partial oxygen crossover through the membrane, degradation can take place also at the anode.

On an experimental scale, the generation of HO• and HOO• radicals can be achieved by a variety of different methods, for instance by direct photochemical [7][8] or photocatalytic degradation of H₂O₂ [9], also by e⁻ irradiation [10][11] or sonolysis [12] of aqueous solutions. In the present work, we chose photolysis of an aqueous H₂O₂ solution as a source of HO• radicals [13] (*Eqn. 1*) which react further *via Eqns. 2 and 3* and other reactions as detailed in *Table 1*. Since aromatic monomers absorb UV radiation as well, care has to be taken to distinguish HO• radical reactions from direct photochemical cleavage.

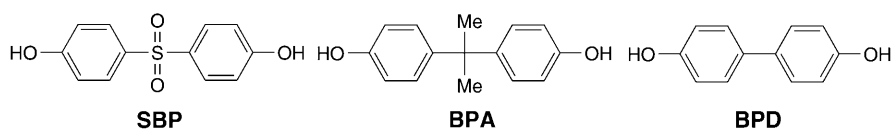


The formation of radical species from the attacked substrate, for instance RH, can occur by H-abstraction, and the polymer-derived R• radicals can initiate a degradation cascade (*Eqn. 4*). The focus of the present work is the chemical degradation which is generally assumed to be based on radical oxidative processes. Electron paramagnetic resonance (EPR) methods are particularly sensitive and suitable for their investigation. In the center of interest are the reaction mechanisms which are accessible *via* the struc-

Table 1. Rate Constants for Reactions of HO• Radicals [22]

Reaction	Rate constant $k/10^9 \text{ M}^{-1} \text{ s}^{-1}$
a: pH > 11.7: $\text{HO}\cdot + \text{HO}_2^- \rightarrow \text{H}_2\text{O} + \text{O}_2^{\cdot-}$	7.5
b: pH < 11.7: $\text{HO}\cdot + \text{H}_2\text{O}_2 \rightarrow \text{H}_2\text{O} + \text{HO}_2\cdot$	0.027
c: $\text{HO}\cdot + \text{O}_2^{\cdot-} \rightarrow \text{HO}^- + {}^1\text{O}_2$	8
d: pH = 11.0: $\text{HO}\cdot + \text{OH}^- \rightarrow \text{O}^{\cdot-} + \text{H}_2\text{O}$	12
e: $\text{HO}\cdot + \text{HO}\cdot \rightarrow \text{H}_2\text{O}_2$	5.5
f: $\text{O}^{\cdot-} + \text{HO}_2^- \rightarrow \text{HO}^- + \text{O}_2^{\cdot-}$	0.4
g: $\text{O}_2^{\cdot-} + \text{O}^{\cdot-} + \text{H}_2\text{O} \rightarrow 2 \text{HO}^- + {}^1\text{O}_2$	0.6

tures of radical intermediates, and the identification of fuel-cell operating conditions which may lead to enhanced radical production. In the present work, these points are addressed by exposing membrane building blocks in solutions to the above intentionally produced oxidative radicals. We investigate the oxidative degradation of 4,4'-sulfonylbis[phenol] (**SBP**), bisphenol A (=4,4'-(1-methylethylidene)bis[phenol]) (=4,4'-isopropylidenebis[phenol]; **BPA**), and [1,1'-biphenyl]-4,4'-diol (**BPD**) in the pH range 0.4–13.9.



The radical intermediates of the HO•-initiated degradation of aromatic-group-containing membranes are of the cyclohexadienyl, benzyl, phenoxy, or ‘ortho-semiquinone’ type. Typical rate constants for reactions with model compounds of relevance in the present context are collated in *Table 2*. They show that HO• addition occurs with rate constants close to the diffusion-controlled limit, H-abstractions are slower by less than an order of magnitude, while O^{•-} can abstract H with a similar efficiency but does not undergo addition. The radicals are observable by EPR and distinguishable by means of their hyperfine splittings and *g* values [6]. Based on the *pK_A* values of H₂O₂ (11.7), HO• (11.9), and HOO• (4.8), the main reactive species below pH 10 is HO•; above pH 13, it is O^{•-} and O₂^{•-}, while at 10 ≤ pH ≤ 13, we have a strongly pH-dependent mixture [6]. Relatively little quantitative information is available for HOO•; but it is known to be significantly less reactive than HO• which reacts by H-abstraction or by addition to unsaturated bonds. The anionic species are less efficient in abstraction reactions but add readily to double bonds or aromatic rings. Under alkaline conditions, radicals are formed by abstraction of H• from the side chains by O^{•-} [6]. Investigations at low pH are particularly relevant for understanding degradation in PEFCs, but one should keep in mind that the chemistry depends strongly on pH, a fact that is highly significant in view of possible pH inhomogeneities in fuel cells under conditions of fuel starvation at high currents [14] or when parts of the anode are flooded by water.

Table 2. Rate Constants for Reactions of HO• and O•⁻ Radicals with Different Substrates [22]

Substrate	Reaction of HO•		Reaction of O• ⁻	
	Product	$k/10^8 \text{ M}^{-1} \text{ s}^{-1}$	Product	$k/10^8 \text{ M}^{-1} \text{ s}^{-1}$
CH ₃ OH	•CH ₂ OH	9.7	•CH ₂ O ⁻	7.5
C ₆ H ₅ OH/C ₆ H ₅ O ⁻	C ₆ H ₅ (OH) ₂	66	C ₆ H ₅ O•	6.5
C ₆ H ₅ CH ₃	C ₆ H ₅ (OH)CH ₂ /C ₆ H ₅ •CH ₂	30	C ₆ H ₅ •CH ₂	21
Benzophenone	adduct	88		
Benzenesulfonic acid	adduct	16		
Benzenesulfonate ion	adduct	30		

2. Experimental. – *Electron Paramagnetic Resonance.* EPR Spectra: Varian E-Line-X-band spectrometer at 2.5 mW microwave power; at r.t. g Values were calculated relative to the Bruker® weak pitch sample ($g=2.0028$). They are accurate to ± 0.0002 units. Second-order effects are within this range of errors for the comparatively small coupling constants observed in our systems, and were neglected. The obtained digital spectra were analyzed by using Microcal Origin®, Version 5.0. Hyperfine splittings were derived from computer simulations with the WINEPR Simphonia program and assigned by comparison with literature values of similar radical systems [15].

Photolysis. At r.t., 4 mm solns. of the monomers (unless otherwise stated) in H₂O/MeOH 1:1 (v/v) (MeOH was added for solubility reasons) were photolyzed within the microwave resonator by a 500-W Hg (Xe) high-pressure mercury-arc lamp (Oriol 66142) in a flat quartz flow cell (0.4 mm × 10 mm × 50 mm). Experiments were also carried out in the presence of 40 mM H₂O₂. Wavelengths below 210 and above 400 nm were eliminated with a filter solution (1.14M NiSO₄/0.21M CoSO₄/0.01M H₂SO₄). A constant flow (8–135 ml h⁻¹) of the solns. through the cell was maintained by a syringe pump. By changing the flow, the residence time within the cavity is varied between 5 and 90 s, so that successive reaction products could separately be focused on.

Doubly distilled H₂O was used, and the pH was adjusted with H₂SO₄ or KOH, by using a digital WTW pH meter (model pH 330) calibrated with commercial buffer solns. Before irradiation, solns. were deoxygenated by bubbling with N₂ for 15 min. H₂O₂ (30% soln.) was obtained from Merck, the BPA, SBP, and BPD monomers from Aldrich.

3. EPR Results and Related Discussion. – 3.1. *4,4'-Sulfonylbis[phenol] (SBP).* SBP is a monomeric building block of the sulfonated PSU. The only species that was detected both in the presence and the absence of H₂O₂ is the *multiplet* of radical **1** with five equidistant EPR lines with relative intensities corresponding to four equivalent protons. Based on its g value (2.0049) and its proton hyperfine coupling constant, there is little doubt that it corresponds to the 'p-semiquinone' radical anion (=cyclohexa-2,5-diene-1,4-dione radical ion (1-)) **1** (Fig. 1, Table 3). SBP has a high molar extinction coefficient ($\epsilon_{296} = 20600 \text{ l mol}^{-1} \text{ cm}^{-1}$ at pH 12.2 and $\epsilon_{260} = 17600 \text{ l mol}^{-1} \text{ cm}^{-1}$ at pH 7.2) so that also in the presence of H₂O₂, the dominant fraction of the light is absorbed directly by the monomer and leads to its cleavage. The signal amplitude increases by a factor of five between the flow rates 8 and 135 ml h⁻¹. At lower flow rates, no signals were detected, indicating that the radical is short lived or the monomer gets depleted.

In the presence of H₂O₂, EPR signals were observed in the range between pH 7.6 and 13.9 (Fig. 2), with a maximum at pH 12.2, near the pK_A of the HO• radicals (11.9) and the pK_A of H₂O₂ (11.7). No signals were observed under acidic or neutral conditions.

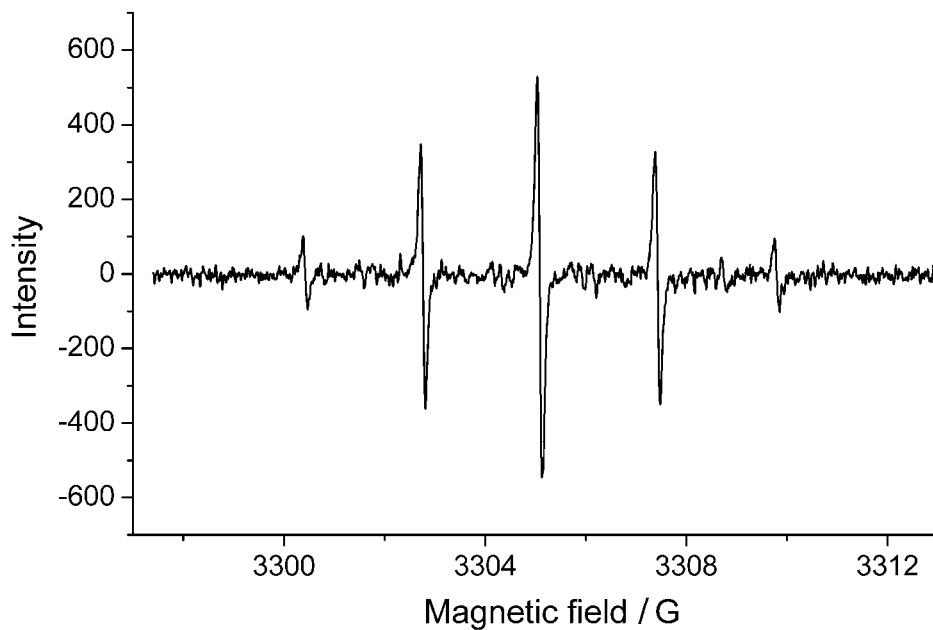


Fig. 1. Experimental EPR spectrum of the 'p-benzoemiquinone' radical anion **1** obtained with SBP at pH 12.2 and 135 ml h^{-1} flow rate

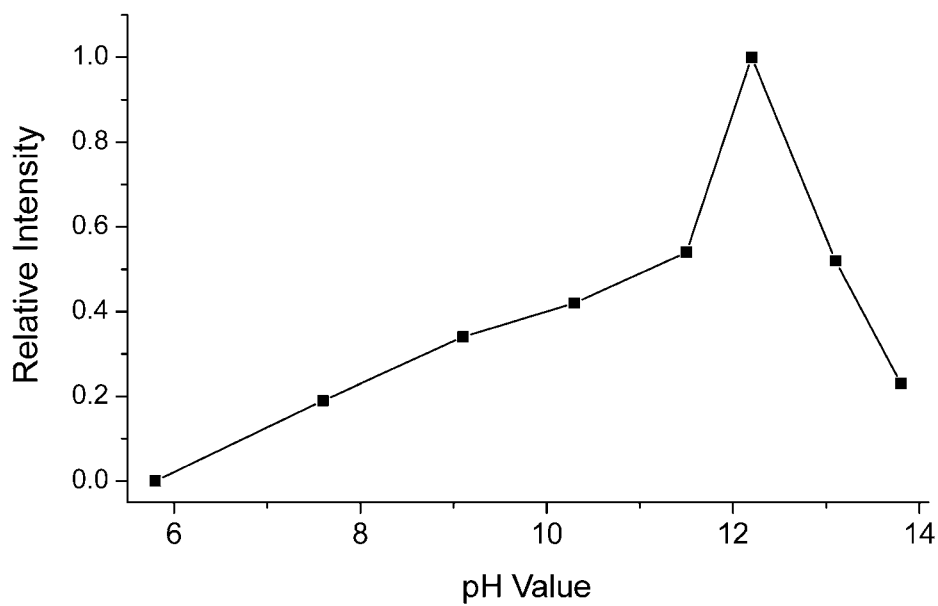


Fig. 2. Relative intensities of the EPR signals of radical **1** observed with SBP at 135 ml h^{-1} flow rate in dependence of the pH value

Table 3. *EPR Parameters of Intermediates in the Reaction of HO• Radicals with Sulfonated Aromatics.* Hyperfine splittings were derived from computer simulations with the WINEPR Simphonia program and assigned by comparison with literature values of similar radical systems [15]. Due to the similarity of all parameters, the structural assignments are somewhat tentative.

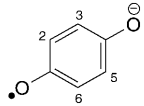
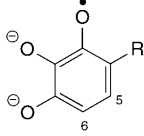
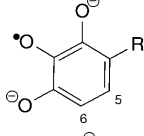
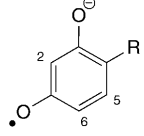
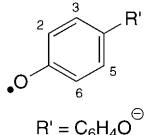
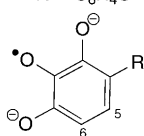
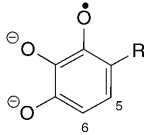
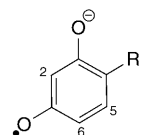
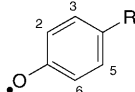
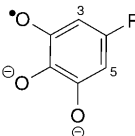
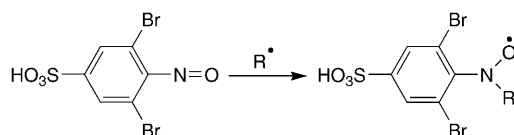
Substrate and conditions	Intermediates		Hyperfine splittings [G]	g
	Nr.	structure		
SBP , pH 12.2, 135 ml h ⁻¹	1		4 H (2,3,5,6): 2.35	2.0049
	BPA , pH 12.0, 135 ml h ⁻¹	1	see above	4 H (2,3,5,6): 2.35
BPD , pH 12.2 (10.3), 135 ml h ⁻¹ , no H ₂ O ₂	2		1 H (5): 3.85 1 H (6): 2.12	2.0048
	R = HOC ₆ H ₄ C(Me) ₂			
	3		1 H (5): 1.52 1 H (6): 3.83	2.0048
	4		1 H (2): 0.64 1 H (5): 0.31 1 H (6): 3.85	2.0048
	5		4 H (2,6,2',6'): 1.84 4 H (3,5,3',5'): 0.92	2.0047
	R' = C ₆ H ₄ O [⊖]			
	6		1 H (5): 1.22 1 H (6): 3.24	2.0044
	R' = HOC ₆ H ₄			
BPD , pH 10.3, 135 ml h ⁻¹ , with H ₂ O ₂	7		1 H (5): 3.25 1 H (6): 1.72	2.0044
	8		1 H (2): 0.50 1 H (5): 0.24 1 H (6): 3.23	2.0044

Table 3 (cont.)

Substrate and conditions	Intermediates		Hyperfine splittings [G]	g
	Nr.	structure		
	9		1 H (2,6): 3.13 1 H (3,5): 0.26	2.0044
	10		1 H (3): 0.26 1 H (5): 0.74	2.0044

Spin trapping is considered to be a powerful tool to visualize short-lived radicals indirectly [16]. In this technique, a diamagnetic compound, called a spin trap, reacts with a primary radical to form a more stable radical that can accumulate to a high enough concentration for an EPR study. In our experiments, 3,5-dibromo-4-nitrosobenzenesulfonic acid (DBNBS) was used as a spin trap, and the reaction that takes place is shown in *Scheme 1*. The advantage of the DBNBS–spin adduct is that it can yield considerable structural information since the primary radical adds directly to the N-atom and remains, therefore, close to the unpaired electron. The applied spin-trap concentration was fixed at 10 mM, all other experimental conditions were identical with the previous measurements. As seen from *Fig. 3*, the observed signals at pH 0.4 consist of a 1:1:1 *triplet* (due to $a_N=13.54$ G) of a 1:2:1 *triplet* (due to 2 equivalent protons with $a_H=8.95$ G). This spectrum clearly arises from the $\cdot\text{CH}_2\text{OH}$ -radical adduct to DBNBS and not from **SBP**. The hydroxyl radicals react first with MeOH, which is to be expected as the initial MeOH concentration (12M) is a factor of 3000 higher than that of **SBP** (4 mM). In view of the high reaction rate of $\text{HO}\cdot$ radicals with MeOH (see *Table 2*), it is clear that in the presence of solvents other than H_2O one should not expect to see products of $\text{HO}\cdot$ reactions with a substrate that is present only in millimolar concentrations. Water-soluble monomers are, therefore, more suitable for experiments involving hydroxyl radicals under acidic conditions. Furthermore, at the higher flow rate (*Fig. 3, b*) a small *triplet* splitting is observed that is due to the H_{meta} of the spin trap molecule DBNBS ($a_H=1.02$ G).

Scheme 1

3.2. *Bisphenol A (BPA)*. **BPA** is a monomeric building block of the sulfonated PSU which, together with PEK, is an alternative for the replacement of the most widely used but expensive perfluorinated *Nafion*[®]. PSU is usually sulfonated by electrophilic sub-

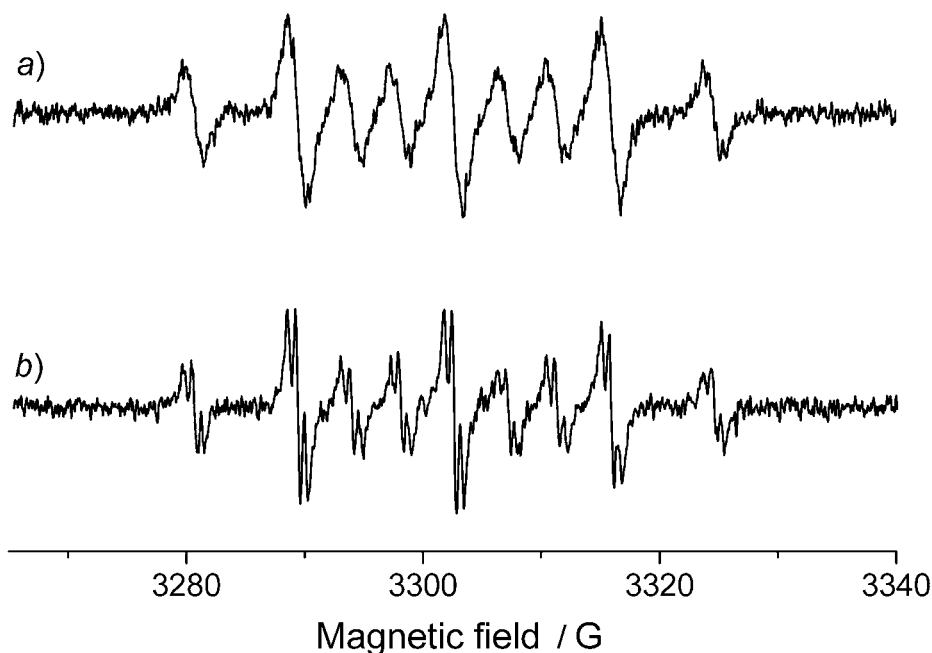


Fig. 3. EPR spectrum of an **SBP/DBNBS/H₂O/MeOH/H₂O₂** mixture at pH 0.4 and at a) a flow rate of 8 ml h⁻¹ and b) a flow rate of 90 ml h⁻¹

stitution at the position *ortho* to the ether bridge of the **BPA** fragment, because this part of the molecule has a high electron density (+*M* effect from the ether bridge, +*I* effect from the linking isopropylidene group), in contrast to the diarylsulfone portion of the monomer repeating unit which has a low electron density due to the electron-withdrawing SO₂ group (–*I* and –*M* effect).

In the absence of H₂O₂, the EPR spectrum shows the same *multiplet* as that found with **SBP**, which is assigned to the '*p*-semiquinone' radical anion **1**. This *multiplet* is superimposed by further lines at lower intensity which appear more strongly in the presence of H₂O₂. **BPA** has a lower absorption coefficient at λ_{max} (ε₂₉₃ = 4000 l mol⁻¹ cm⁻¹ at pH 12.0) than **SBP** but absorbs strongly at shorter wavelength (ε₂₄₂ = 16960 l mol⁻¹ cm⁻¹).

In the presence of H₂O₂, the EPR spectrum at pH 12 and flow rate 135 ml h⁻¹ is quite different (Fig. 4). H₂O₂ or its anions are obviously photolyzed, most likely at wavelengths near 267 nm where there is a window between the above absorption bands. The spectrum is nearly symmetric and consists of two groups of lines, which, based on their intensities and their variation with experimental conditions, cannot be assigned to a single radical. From simulations and comparison of the coupling constants with literature values [15], it was concluded that the observed spectrum consists of a superposition of the four different radical species **1–4** with almost identical *g* values (Table 3). Due to the mesomerism, the largest coupling constants are in the *ortho*- and *para* positions relative to the phenoxy radical center.

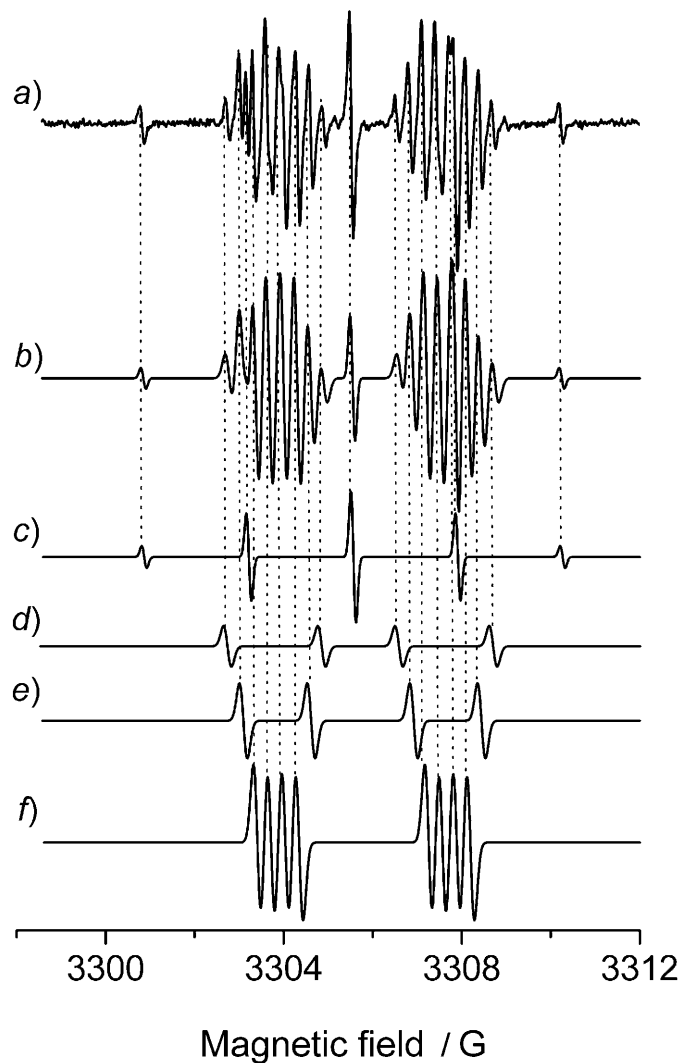


Fig. 4. a) Experimental EPR spectrum obtained with **BPA** at pH 12 and at 135 ml h^{-1} flow rate, b) simulation of the spectrum for the sum of radicals **1–4**, c) simulation of the spectrum of radical **1** (33%), d) simulation of the spectrum of radical **2** (5%), e) simulation of the spectrum of radical **3** (14%), and f) simulation of the spectrum of radical **4** (48%)

BPA is a symmetric compound; therefore, only one aromatic ring will be taken into consideration. No coupling through the Me_2C group is observed (*Table 3*). Radical **1** is the same '*p*-semiquinone' radical anion as observed in the absence of H_2O_2 . It arises from the fraction of light that is absorbed directly by the monomer. For the other species, the number of *doublet* splittings in the spectrum shows that there are only two H-atoms for radicals **2** and **3**, and three for radical **4**. The lack of H-couplings within aro-

matic rings suggests that secondary reactions like further hydroxylation or dimerization of the monophenoxy radicals occur. The latter can be excluded at higher flow rates, because of the absence of the expected additional splittings from the H-atoms in the neighboring ring. At lower flow rates, the spectra are different (Fig. 5), but in contrast to Fig. 3 where additional structure appears at the higher flow rate, we have more and narrower lines at low flow rate. This points to an explanation involving primary radicals predominantly at high flow rates and secondary ones at lower rates with corresponding extended residence time in the EPR-active zone of the cell. Due to dimerization, additional smaller coupling constants appear. Coupling of phenoxy radicals forming either phenoxy-, phenol- or biphenyl-like radicals has previously been described [17][18], but the possible formation of consecutive new monomeric species should nevertheless not be excluded.

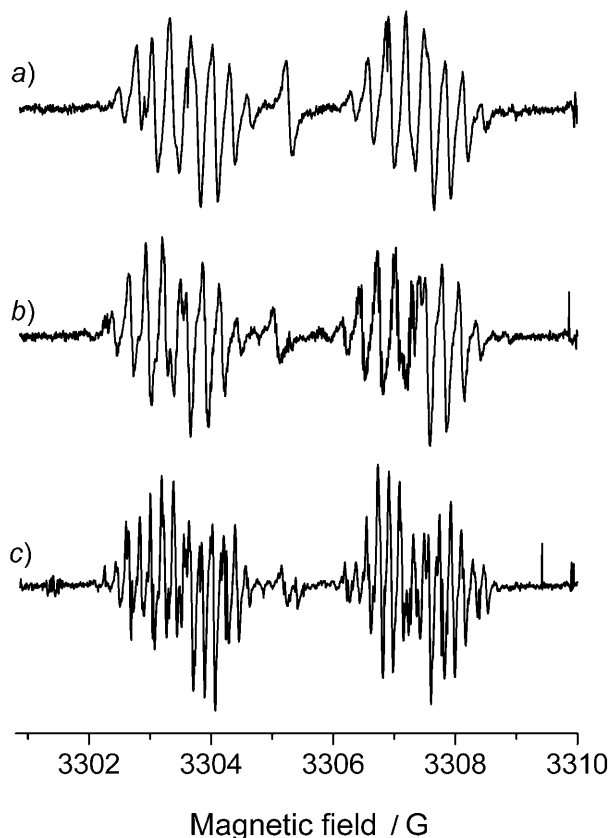


Fig. 5. EPR Spectra obtained with BPA at pH 12 and at different flow rates: a) 90 ml h^{-1} ; b) 20 ml h^{-1} and c) 8 ml h^{-1}

An additional contribution to the formation of higher-substituted products may be due to the increased absorption coefficients of H_2O_2 solutions under alkaline conditions (pH 0.45: $\epsilon_{230} = 42 \text{ l mol}^{-1} \text{ cm}^{-1}$ for H_2O_2 ; pH 12.6: $\epsilon_{230} = 317 \text{ l mol}^{-1} \text{ cm}^{-1}$ for HOO^-).

The signal amplitudes arising from the four observed radicals depend only slightly on the flow rates (not shown) and do not permit a clear conclusion as regards radical-formation mechanism. For the determination of the relative intensities, a clear EPR line, not overlapping with other signals, was chosen for each individual radical. Its intensity ($1/2 \cdot \Delta H$ (line width) \cdot signal intensity) was used to determine the cumulative intensity of all lines of the individual radical.

It is clearly seen that all four radical species **1–4** exist in a specific pH range between pH 9 and 14 (Fig. 6). The relative concentrations of the four radicals remain the same, and a maximum of the absolute intensity is adopted at pH 11.8. This behavior will be discussed in Sect. 4.2.

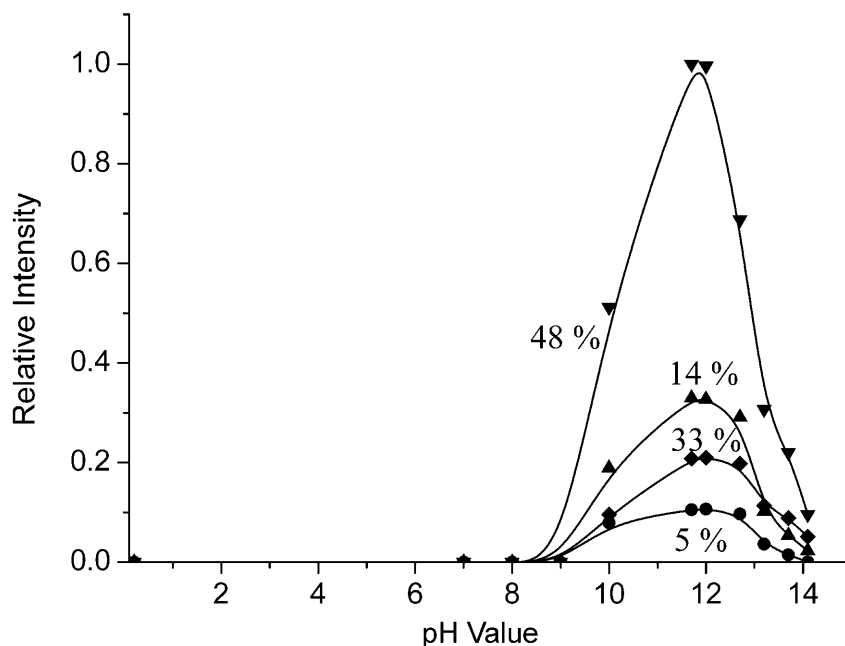


Fig. 6. Relative intensities of the EPR signals of the radicals **1** (\blacklozenge), **2** (\bullet), **3** (\blacktriangle), and **4** (\blacktriangledown) observed with **BPA** at 90 ml h^{-1} flow rate in dependence on the pH value

Experiments with the DNBNS spin trap at pH 0.4 and a flow rate of 90 ml h^{-1} led to the same spectrum (not shown) as observed with **SBP**, arising from the $\cdot\text{CH}_2\text{OH}$ radical. At the given concentration, **BPA** cannot successfully compete for $\text{HO}\cdot$ with the MeOH solvent. Nevertheless, a change of color of the solution demonstrates that photochemical reactions do occur.

3.3. *[1,1'-Biphenyl]-4,4'-diol (BPD)*. **BPD** has a strong absorption band at 286 nm ($\epsilon_{286} = 32400 \text{ l mol}^{-1} \text{ cm}^{-1}$ at pH 11.7) which shifts to 262 nm and somewhat lower absorption at pH 10.35. In the absence of H_2O_2 , the experimental EPR spectrum of 2 mM **BPP** consists of a *multiplet* with 13 equidistant lines. The intensity distribution is compatible with two sets of four equivalent protons with coupling constant which are a factor of two different (0.92 G and 1.84 G) but not with 12 equivalent protons. It is

conceivable that this spectrum is due to the ‘*p*-dipheno-semiquinone’ anion radical (=4-(4-oxocyclohexa-2,5-dien-1-ylidene)cyclohexa-2,5-dien-1-one radical ion (1–)) **5** which may be formed by photooxidation followed by deprotonation of **BPD**, although a somewhat different set of coupling constants (0.56 and 2.25 G, the sum of which is nearly the same as that of the present observation) has been reported for this species in the literature [19]. The spectrum is considerably weaker near pH 10 than at pH 12.2.

In the presence of H_2O_2 , the 13-line EPR spectrum of radical **5** (Fig. 7, a) is absent, and the observed EPR signals are strongly pH dependent (Fig. 7, b–e), in a similar sense as seen before with **BPA**. Simulating the experimental EPR spectrum at pH 10.3 and flow rate 135 ml h^{-1} , and comparing the coupling constants with literature values [15], it was concluded that the observed spectrum consists of five different, simultaneously appearing radical species with identical *g* values (Table 3; details are reported in [20]). The fractions which are determined by matching the intensities in the simulation are 26% for radical **6**, 14% for radical **7**, 35% for radical **8**, 17% for radical **9**, and

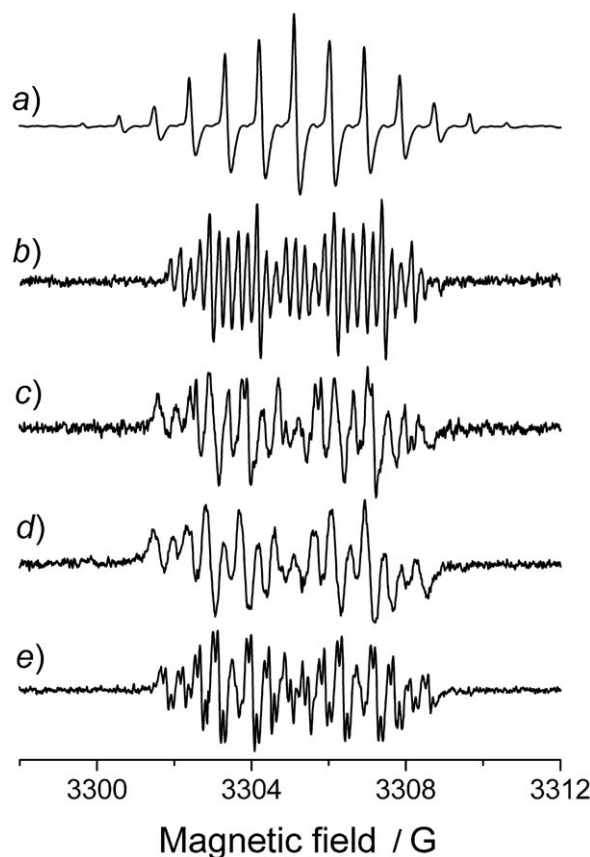


Fig. 7. EPR Spectra obtained with **BPD** acquired at 135 ml h^{-1} flow rate and a) at pH 12.2 in the absence of H_2O_2 , b) at pH 10.3 in the presence of H_2O_2 , c) at pH 11.3 in the presence of H_2O_2 , d) at pH 12.2 in the presence of H_2O_2 and e) at pH 13.0 in the presence of H_2O_2

8% for radical **10**. The number of *doublet* splittings shows that there are only two H-atoms for radicals **6**, **7**, and **10**, and three for radical **8**. The lack of H-couplings within aromatic rings suggests that secondary reactions like further hydroxylation of the monophenoxy radicals occur. Only radical **9** possesses four H-atoms.

It should be noted that there is a pronounced change in the spectra as the pH increases from 10.3 to 13.0. The well-resolved spectrum with 27 almost equidistant lines at pH 10.3 (*Fig. 7, b*) transforms into a less well resolved 16-line spectrum at pH 12.2 (*Fig. 7, d*). On further increase to pH 13.0, most but not all of the lines split into 0.1-G *doublets*. The total width and one dominant hyperfine splitting of *ca.* 3.2 G remain roughly constant. It is likely that the changes reflect protonation equilibria, but the details remain elusive.

4. Discussion. – 4.1. *Aspects of Direct Photolysis.* While it is clear that **SBP** and related sulfones are degradable by UV light, little is known about the mechanism. The formation of the '*p*-benzosemiquinone' radical anion establishes that the molecule is cleaved in *α*-position to the sulfone group, which is conceivable in analogy to the known *Norrish*-type-II cleavage of ketones under conditions where photoreduction is suppressed. It is less clear though why this does not work under acidic conditions where only the spin-trap adduct of the hydroxymethyl radical is observed. These conditions may point to the involvement of HO[•] to trap the phenyl fragment and produce the 'semiquinone'. It is furthermore noteworthy but not so rare that the counter radical from photolysis is not observed, a fact that may be related to a short lifetime.

It is known that **BPA** photoionizes at 308 nm to give a bis-phenoxy radical and a solvated electron [21]. It is perhaps the shorter wavelength employed here which leads to cleavage of the C–C bond in the bridge to provide the '*p*-benzosemiquinone' radical. Again, the latter is not observed under acidic conditions, suggesting that an analogous mechanism as suggested for **SBP** is operative.

The **BPD** does not cleave but photo-oxidizes to the '*p*-dipheno-semiquinone' radical anion. There can be little doubt about the nature of this species, and it is unclear why the spectrum is different from the one reported in [19].

4.2. *Formation of Phenoxy- and 'Semi-quinone' Radicals and the Origin of Its pH Dependence.* The pH dependence shown by the HO[•] radical in reactions with substituted aromatic hydrocarbons is related to its deprotonation (pK_A 11.9) under alkaline conditions [22]. The resulting O^{•-} radical possesses only negligible tendency to add to the aromatic ring, so that at pH values exceeding the pK_A of HO[•], H-abstraction from the substituents leading to phenoxy radicals is expected to be the predominating process.

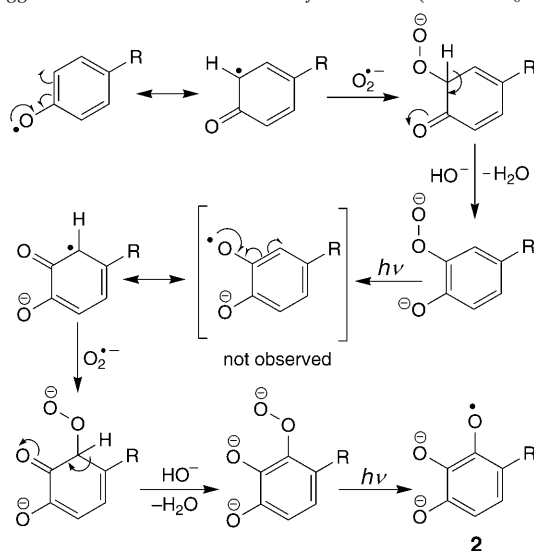
As detailed in *Sect. 3.1*, the presence of MeOH as a solvent scavenges HO[•] efficiently so that no addition to the aromatic rings is observed.

It is remarkable that the maximum formation of phenoxy radicals from **BPA** and **SBP** occurs in the pH range close to the pK_A of the HO[•] radicals (11.9) and of H₂O₂ (11.7). This has been shown to be due to the rates of formation of O₂^{•-} and of ¹O₂ which are proportional to the products of the rate constants and the pH dependent concentrations of the reactants [6]. H-Abstraction from the deprotonated form HO₂⁻ is *ca.* 300 times faster than from H₂O₂ (see *Table 1, Reactions a and b*) [22]. The resulting O₂^{•-} undergoes oxidation by HO[•] or O^{•-}, so that oxygen is formed *in-situ* in the reaction sol-

utions (see Table 1, Reactions c and g) [22]. Oxygen formed by this reaction has been reported to be of a singlet character ($^1\text{O}_2$) [23]. This is obviously true, since $^3\text{O}_2$ would lead to an extensive spin exchange and thus to the loss of hyperfine structure in the EPR spectra, in contrast to our observations (see, e.g., Fig. 7, e). The evolution of oxygen is apparent by the bubble formation in the photolysis cell at high pH.

$\text{O}_2^{\cdot-}$ plays a determining role for the production of all radicals formed at high pH. Moreover, $\text{O}^{\cdot-}$ and $\text{O}_2^{\cdot-}$ are radicals with nucleophilic nature that leads to H abstraction from phenolic OH substituents, thus producing the primary phenoxy radicals. $\text{O}_2^{\cdot-}$ can also attach directly to the aromatic ring. A suggested reaction mechanism is displayed in Scheme 2. As may be evidenced by mesomeric structures, there is a higher probability that the unpaired electron is at the *ortho* or *para* position to the primary oxy group. The $\text{O}_2^{\cdot-}$ attacks the *ortho* position (the *para* position is sterically hindered), and the proton is readily split off due to rearomatization under alkaline conditions. The O–O bond is broken by irradiation with UV light, and an intermediate is formed which reacts very fast *via* the same reaction pathway and cannot be detected at the used flow rate. The formation of other radicals may be rationalized by a similar mechanism.

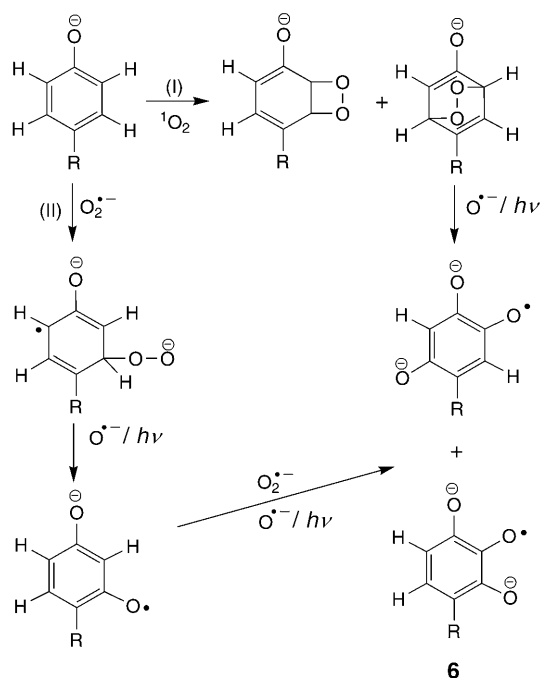
Scheme 2. Suggested Formation Mechanism of Radical 2 ($\text{R}=\text{HOC}_6\text{H}_4\text{C}(\text{Me})_2$) [26]



Alternatively, radicals may be formed by reaction with singlet oxygen. $^1\text{O}_2$ is known to have a pronounced tendency to undergo [2+2] and [2+4] cycloadditions to organic C=C bonds [24] [25]. Thus, the addition of $^1\text{O}_2$ directly to the aromatic ring leads to the formation of the observed dioxy-substituted radicals. The $\text{O}_2^{\cdot-}$ radical is formed according to Reactions a and f (Table 1), and in contrast to its protonated form (HOO^{\cdot} , $\text{p}K_{\text{A}}$ 4.8), it also shows tendencies to add directly to the aromatic rings and hence must be considered as an intermediate to phenoxy-radical formation (Scheme 3).

Strongly deactivating substituents such as SO_3^- and SO_2 which exert a $-I/-M$ effect direct nucleophilic substitution to the *meta* position. An oxy substituent which is

Scheme 3. Possible Formation Mechanism of Radical **6** and Further Dioxy-Substituted Species (R = HOC₆H₄) [13][24][25]



strongly activating, with a +I+M effect, favors further substitution at *ortho* and *para* positions.

4.3. Relevance for Fuel-Cell Membranes. The proton-exchange membrane is a key component of the PEFC. In the current state of technology, perfluorinated membrane materials such as *Nafion*[®] (DuPont, USA) and *Flemion*[®] (Asahi Kasei, Japan) are used predominantly due to the attractive conductivity and chemical stability of these materials. However, for market introduction of fuel-cell products to take place, cost-competitive membrane technology has to be available.

The present work investigates monomeric membrane building blocks under conditions which are not in every aspect those in fuel cells. However, when high currents are drawn, this can give rise to significant pH inhomogeneities as a consequence of local variations in catalytic activity and in proton conductivity. Oxidative degradation of polymers is usually a radical process which involves attack of the hydroxyl and the hydroperoxyl radicals, HO[•] and HOO[•]. Both radicals are intermediates of the oxygen reduction in a fuel-cell process, and since hydrogen peroxide has been detected as a trace by-product of the fuel-cell reaction, it is plausibly assumed that attack of these two radicals is an important degradation pathway of the proton-conducting polymer membrane. At $\text{pH} \geq \text{p}K_{\text{A}}$ of HO[•] and H₂O₂, reactions between the model compounds and O₂^{•-} or $^1\text{O}_2$ are the most probable ways to the phenoxy and ‘semiquinone’ radicals observed in this pH range in our EPR spectra. It was shown in previous work [6] that the dominating reaction is the addition of HO[•] to the aromatic rings, preferentially in the *ortho*-position

to alkyl and RO substituents (since in sulfonated PEK, PSU, PS, and ETFE or FEP-g-PSA, the *para* position is substituted and thus blocked). The present study focuses on the case in which $O_2^{\cdot-}$ or 1O_2 are the damaging species above pH 11.7, and in which the dominating reaction is that with the aromatic ring.

It is normally essential for the EPR technique that the samples are deoxygenated. 3O_2 reacts with radicals by spin exchange, but in particular it adds and thus forms dioxy radicals which are more difficult to see. Under fuel-cell operating condition there is plenty of 3O_2 present, at least near the cathode, but 1O_2 is not expected to form. Only under local pH inhomogeneities, 1O_2 formation should also be considered as a possible reaction pathway especially at $pH \geq 11.7$. In the presence of both HO^{\cdot} radicals and oxygen, complete degradation of the aromatic rings can be achieved within a few hours [13]. In view of this, the perfluorinated *Nafion*[®] which is much more inert has an inherent advantage over the new membranes based on aromatic hydrocarbons.

It is known that the sulfone group has a deactivating role. Thus, in comparison with the other monomeric building blocks, **SBP** has an advantage in terms of chemical stability towards HO^{\cdot} addition. Furthermore, blocking of the aromatic ring by suitable substitution, for example by F-atoms, limits the HO^{\cdot} addition reactions. SO_3^- Substituents are introduced to give rise to proton conductivity, but as an additional benefit, they reduce the activity of the aromatic ring towards HO^{\cdot} hydroxyl radical addition (see *Table 2*). Another possibility, as briefly mentioned in the introduction, is the polymer blending. In DMFC, the most promising fuel-cell performance is obtained on membranes based on sPEKs and their blends, and recent results indicate power density as good as the ones obtained with *Nafion*[®], with the difference that polyaromatic membranes can be restarted over several weeks without degradation at temperature $> 100^\circ$ [1].

In addition, future *in situ* EPR experiments by using a complete MEA in an operating fuel cell are planned to investigate the membrane under realistic and forced running conditions. Here, radicals are no longer generated photolytically. Instead, it will be the key aim of these investigations to see whether the same radicals which are intermediates of the oxygen reduction can be liberated from the catalyst surface and cause their havoc on the membrane. Furthermore, spin-trap agents will be used to make elusive radicals visible. The novel method for a direct investigation of radical processes in a running fuel cell is already developed in our group, and first results have been reported [27].

5. Conclusions. – The 4,4'-sulfonylbis[phenol] (**SBP**) and bisphenol A (**BPA**) can be cleaved by UV photolysis in aqueous methanol solution at $pH > 10$ to give '*p*-benzosemiquinone' radical anions, whereas [1,1'-biphenyl]-4,4'-diol (**BPD**) does not cleave but gives the '*p*-dipheno-benzosemiquinone' radical anion. If in addition hydrogen peroxide is present, this opens new reaction pathways. At $pH < 10$, H_2O_2 is photolyzed to give HO^{\cdot} radicals which react more readily with the MeOH solvent than with the substrate. The hydroxymethyl-radical intermediate can, however, be trapped by spin-trap molecules. Since both H_2O_2 and HO^{\cdot} deprotonate near pH 11.7, the new reactive species is $O^{\cdot-}$ which can abstract H-atoms but shows little tendency for addition, but in particular, $O_2^{\cdot-}$ or 1O_2 are formed which are held mainly responsible for the formation of phenoxy- and semiquinone-type aromatic polyoxy radicals. For fuel cells with polymer-mem-

brane electrolytes, this means that high pH values which may occur under conditions of fuel starvation and large inhomogeneities are very damaging and lead to rapid degradation of the membrane.

We greatly acknowledge financial support by the *Deutsche Forschungsgemeinschaft* (RO 1249/4-1) and the *Sino-German Center* in Beijing. The *Varian* EPR spectrometer on which the present work was performed was donated by Prof. *H. Fischer*.

REFERENCES

- [1] J. Roziere, D. Jones, *Annu. Rev. Mater. Res.* **2003**, 33, 503.
- [2] J. A. Kerres, *J. Membr. Sci.* **2001**, 185, 3.
- [3] H. Wang, G. A. Capuano, *J. Electrochem. Soc.* **1998**, 145, 780.
- [4] F. N. Büchi, B. Gupta, O. Haas, G. G. Scherer, *Electrochim. Acta* **1995**, 40, 345.
- [5] W. Liu, D. Zuckerbrod, *J. Electrochem. Soc.* **2005**, 152, A1165.
- [6] G. Hübner, E. Roduner, *J. Mater. Chem.* **1999**, 9, 409.
- [7] S. Lunak, P. Sedlak, *J. Photochem. Photobiol., A* **1992**, 68, 1.
- [8] N. Jacob, I. Balakrishnan, M. P. Reddy, *J. Phys. Chem.* **1977**, 81, 17.
- [9] E. J. Wolfrum, D. F. Ollis, *Aquat. Surf. Photochem.* **1994**, 2, 451.
- [10] P. Neta, M. Z. Hoffmann, M. Simic, *J. Phys. Chem.* **1972**, 76, 847.
- [11] K. Eiben, R. W. Fessenden, *J. Phys. Chem.* **1971**, 75, 1186.
- [12] K. Makino, M. M. Mossoba, P. Riesz, *J. Phys. Chem.* **1983**, 87, 1369.
- [13] H. Kaczmarek, L. A. Linden, J. F. Rabek, *Polym. Degrad. Stab.* **1995**, 47, 175.
- [14] E. Roduner, S. Schlick, 'Degradation of Polymer Membranes Used in Fuel Cell Applications', in 'Advanced EPR Methods in Polymer Research', Ed. S. Schlick, John Wiley & Sons, New York, 2006, Chapt. 8.
- [15] 'Landolt-Boernstein, New Ser. II', Springer-Verlag, Berlin, 1977.
- [16] E. G. Janzen, *Acc. Chem. Res.* **1971**, 4, 31.
- [17] M. Ye, H. Schuler, *J. Phys. Chem.* **1989**, 93, 1898.
- [18] H. I. Joschek, S. I. Miller, *J. Am. Chem. Soc.* **1973**, 88, 3273.
- [19] F. R. Hewgill, M. C. Pass, *Aust. J. Chem.* **1985**, 38, 537.
- [20] S. Mitov, B. Vogel, E. Roduner, J. Kerres, M. Hein, D. Xing, F. Schönberger, H. Zhang, X. Zhu, V. Gogel, L. Jörissen, in preparation.
- [21] C. M. R. Clancy, M. D. E. Forbes, *J. Phys. Chem. A* **2001**, 105, 9869.
- [22] G. V. Buxton, C. L. Greenstock, W. P. Helman, A. B. Ross, *J. Phys. Chem. Ref. Data* **1988**, 17, 513.
- [23] R. Ruggiero, A. E. H. Machado, A. Castellan, S. Grelier, *J. Photochem. Photobiol., A* **1997**, 110, 91.
- [24] I. Saito, S. Kato, T. Matsuura, *Tetrahedron Lett.* **1970**, 11, 239.
- [25] D. R. Kearns, *Chem. Rev.* **1971**, 71, 395.
- [26] C. Went, 'Ionic Organic Mechanisms', in 'Dimensions of Science', Ed. J. J. Thompson, Macmillan Education Ltd., London, 1986.
- [27] A. Panchenko, H. Dilger, J. Kerres, M. Hein, A. Ulrich, T. Kaz, E. Roduner, *Phys. Chem. Chem. Phys.* **2004**, 6, 2891.

Received May 2, 2006